Overview of Studies on Microbunching Instability (μBI)

Rui Li

CASA, Jefferson Lab

Outline

- Introduction
- Physical model of μBI due to CSR and LSC
- Experimental Observations
- μBI with more refined model of LSC and CSR
- Mitigation Schemes and applications of μBI
- Summary

1. Introduction

- Microbunching Instability
  - Longitudinal density modulation in the electron bunch which is amplified through
    - energy modulation via collective interaction such as space charge and CSR
    - dispersion induced R_{56}
  - This can meanwhile cause increase of uncorrelated energy spread and deterioration of beam phase space quality

This phenomena can take place in both kind devices:

- Single pass linac device including bending systems
- Storage ring

Saldin, Schneidmiller, M.V. Yurkov, NIM. A **490**, 1 (2002).

Illustration of the Microbunching Process

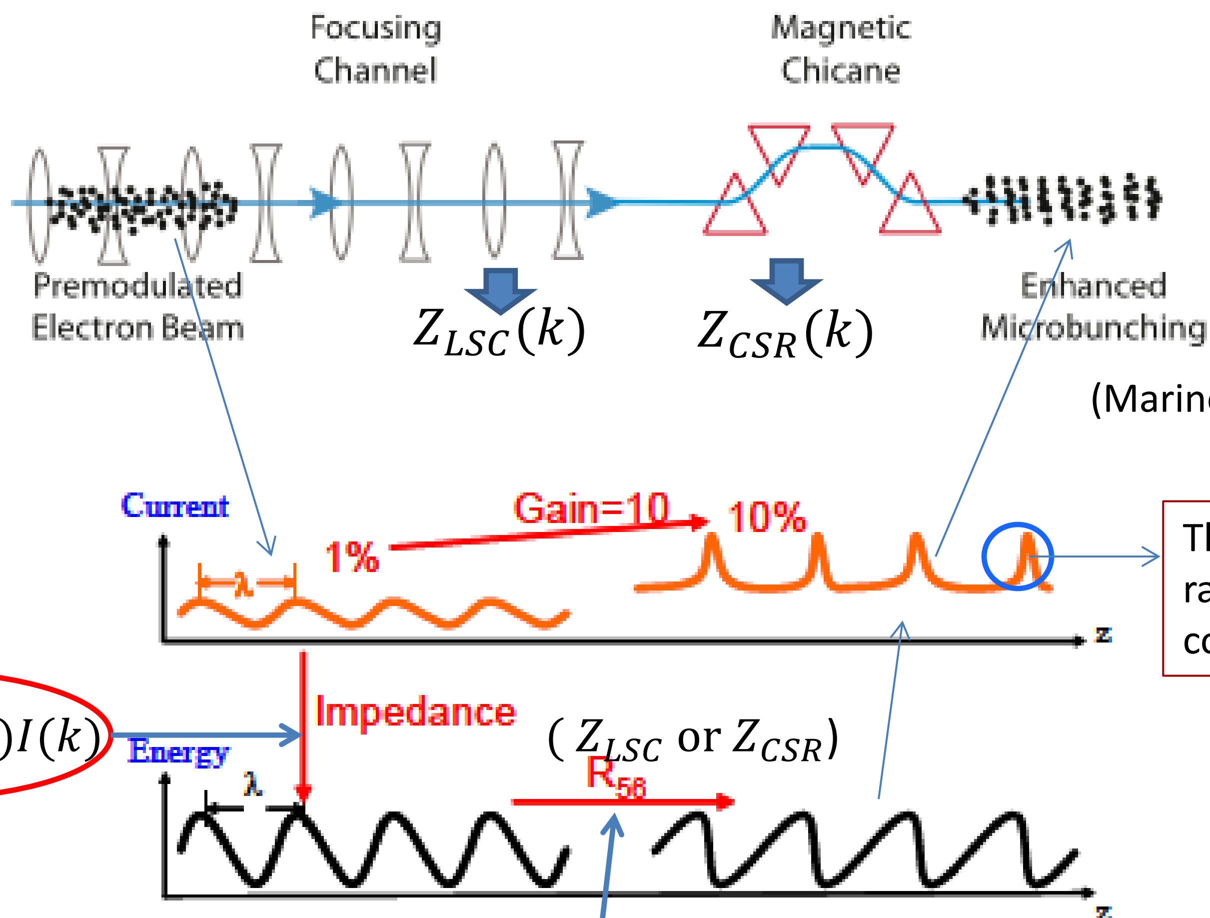

Figure 1: An illustration of microbunching instability in a bunch compressor.

(Marinelli, 4th μBI Workshop)

These particles can radiates together, constructive in phase

$E_z(k) = Z(k)I(k)$

(Z. Huang, SLAC-PUB-11597)

bunching factor:

$b(k) = \frac{I(k)}{ec}$

$z = z_0 + R_{56}\,\delta_0$

μBI impact on machine performance

- Coherent optical transition radiation (COTR)

PHYSICAL REVIEW SPECIAL TOPICS - ACCELERATORS AND BEAMS **11**, 030703 (2008)

Commissioning the Linac Coherent Light Source injector

R. Akre, D. Dowell, P. Emma, J. Frisch, S. Gilevich, G. Hays, Ph. Hering, R. Iverson, C. Limborg-Deprey, H. Loos, A. Miahnahri, J. Schmerge, J. Turner, J. Welch, W. White, and J. Wu
SLAC, Stanford, California 94309, USA

XI. UNEXPECTED PHYSICS

During beam emittance studies downstream of BC1, a strong enhancement of the optical signal from the OTR foils was observed with extreme bunch compression. The

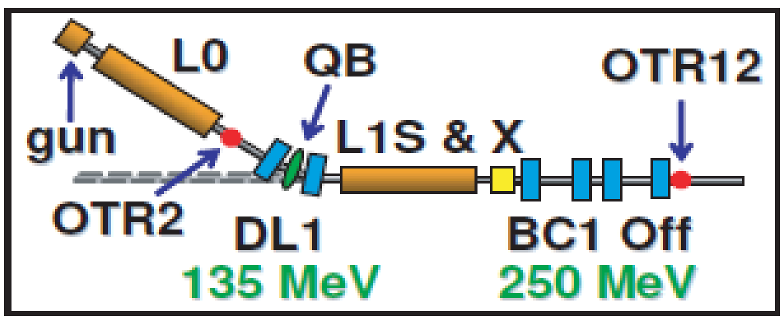

Figure 1: LCLS injector layout showing OTR2, DL1 and OTR12 for the COTR experiment when BC1 is off.

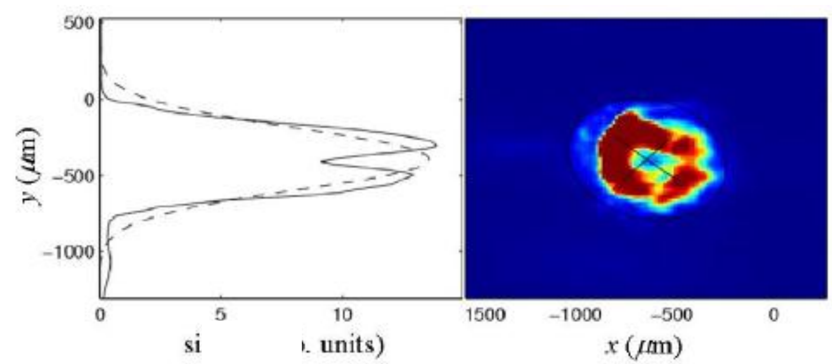

FIG. 43. (Color) An image of the COTR radiation after BC1 observed with extreme bunch compression.

The Development of Microbunching Instability

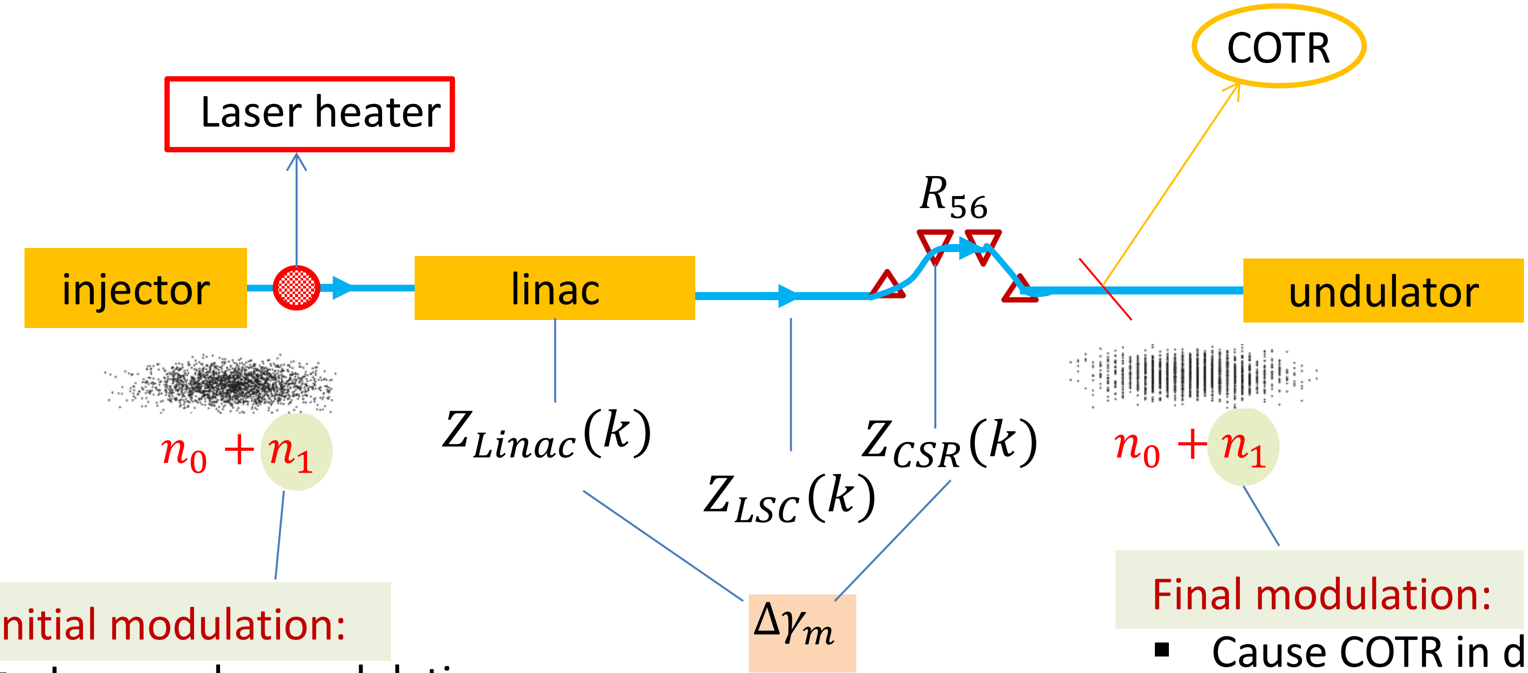

Initial modulation:

- Laser pulse modulation
- Shot noise

Final modulation:

- Cause COTR in diagnostics
- Degrade FEL performance

Important factors at play:

- σ_{un}
- Initial modulation
- $\vec{F}^{col}$ or $Z(k)$
- Phase space rearrangement

uBI characterization:

- Bunching factor: $b(k) =< e^{-ikz_i} >$
- Gain : $G(k) = \left|\frac{b_f(k)}{b_0(k)}\right|$
- $\langle |b(k)|^2 \rangle$

Important factors in Microbunching Instabilities

- σ_{un} → Play a role of Landau damping
  Can be modified by introducing heater device

- Initial modulation → Need careful description of shot noise distribution or initial density modulation

- $\vec{F}^{col}$ or $E_z(k)$ → Need careful modeling of LSC or CSR (1D, 2D, 3D)

- Phase space rearrangement → Transverse and longitudinal optics, thermal emittance effect

Goals of Microbunching Studies

- Develop theories which can represent the fundamental mechanisms of the process

- Develop numerical modeling which can be benchmarked with theories for ideal cases, and can predict and explain experimental observations

- Mitigate the instability, or even better, making use of it

2. 1D Model of Microbunching Instabilities: Theory and Simulations

- CSR induced μBI
  - 1D model of CSR force
  - Gain of microbunching instability

- LSC induced μBI
  - 1D model of LSC force
  - Gain of microbunching instability

CSR Interaction in Bends (1D model)

Particles on a circular orbit interact through Lienard-Wiechert field

$$\vec{E} = e\left(\frac{\hat{n}-\vec{\beta}}{\gamma^2\left(1-\vec{\beta}\cdot\hat{n}\right)^3 R^2}\right)_{ret} + \frac{e}{c}\left(\frac{\hat{n}\times\left(\hat{n}-\vec{\beta}\right)\times\dot{\vec{\beta}}}{\left(1-\vec{\beta}\cdot\hat{n}\right)^3 R^2}\right)_{ret}$$

$$\frac{dp_k}{dt} = \sum_{i=1}^{N}(E + \beta \times B)$$

$$\vec{B} = \hat{n}\times\vec{E}$$

1D free-space steady-state CSR impedance:

- neglect transverse CSR force
- neglect effect of transverse size $\left(R^{1/3}\ \lambda^{2/3} \gg \sigma_x\right)$
- negligible transient effect
- negligible shielding effect
- $\lambda \gg R/\gamma^3$

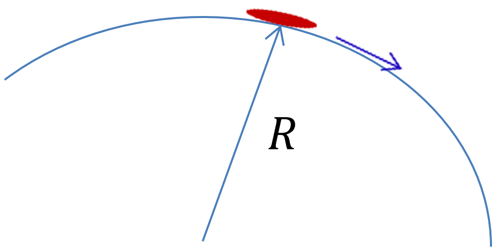

$$Z_{CSR}(k) = -i\ A\ \frac{c\ Z_0}{4\ \pi}\ \frac{k^{1/3}}{R^{2/3}} \qquad (A = 1.63i - 0.94)$$

CSR Driven μBI During Bunch Compression

- **Process**

  Density modulation

  $Z_{CSR}(k)$ ↓ ↑ R_{56}

  Energy modulation

- **Assumptions**
  - 4D optics for particle dynamics
  - CSR field based on 1D bunch

- **Approach**
  - Linearized Vlasov equation for 4D phase space
  - Iterative solution

$$b(k(s);s) = b_0(k(s);s) + \int_0^s d\tau K(\tau,s) b(k(\tau);\tau)$$

$$\text{kernel } K(\tau,s) = ik(s)R_{56}(\tau \to s)\frac{I(\tau)}{\gamma I_A} Z(k(\tau)) \times \underbrace{\exp(\ldots\varepsilon,\sigma_\delta\ldots)}_{\text{Landau damping}}$$

- **Results**

$$\text{gain}(k) = \frac{b(k(s),s)}{b_0(k(s),s)}$$

(μBI gain in chicane is not large because of emittance caused longigudinal smearing via R_{51} and R_{52})

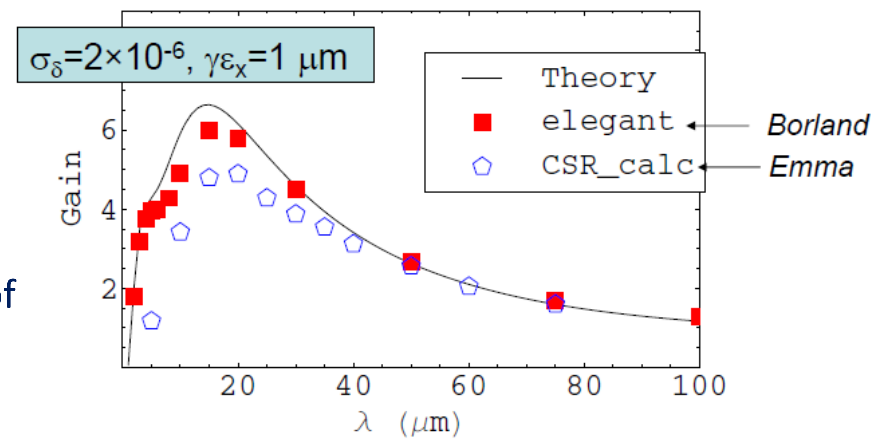

M. Borland et al., NIM A483 (2002)268

S. Heifets, G. Stupakov and S. Krinsky, PRST-AB 5 (2002) 064401

Z. Huang and K.-J. Kim, PRST-AB 5 (2002)074401

Space Charge (1D) and Linac Impedance

$$E_z(x) = \frac{e}{4\pi\epsilon_0}\sum_j^N \frac{\gamma_0(z-z_j)}{[(x-x_j)^2+(y-y_j)^2+\gamma_0^2(z-z_j)^2]^{3/2}}$$

Longitudinal space charge impedance averaged over transverse cross section (round Gaussian beam with universe transverse cross section)

$$Z_{LSC}(k) = \frac{iZ_0}{\pi k {r_b}^2}\left[1 - \frac{kr_b}{\gamma} K_1\left(\frac{kr_b}{\gamma}\right)\right]$$

$$\approx \begin{cases} \dfrac{iZ_0}{\pi k {r_b}^2} & \left(\dfrac{kr_b}{\gamma} \gg 1\right) \quad \text{(wide beam, low energy)} \\ \dfrac{iZ_0 k}{4\pi\gamma^2}\left(1 + 2\ln\dfrac{\gamma}{kr_b}\right) & \left(\dfrac{kr_b}{\gamma} \ll 1\right) \quad \text{(thin beam, high energy)} \end{cases}$$

J. Rosenzweig et al. , TESLA-FEL-96-15 (1996)

Z. Huang and T. Shaftan, SLAC-PUB-9788 (2003)

Space Charge Driven μBI (linac+drift+chicane)

- **Process**

Density modulation

(in drift + linac) $Z_{LSC}(k) \downarrow \quad \uparrow R_{56}$ (in chicane)

Energy modulation

- **Assumptions**
  - In drift, longitudinal density frozen, space charge oscillation negligible
  - Angular spread do not spoil MBI

- **Approach**
  - Calculate gain using bunching factor at initial and final path length
  - Mapping from (z_0, δ_0) to (z_f, δ_f), linear expansion using $|k_f R_{56} \delta_m| \ll 1$

- **Results**

$$\Delta\gamma_m = -\frac{I_0 b_0(k)}{I_A} \int_0^L ds \, \frac{4\pi Z(k_0; s)}{Z_0}$$

$$G \approx \frac{I_0}{\gamma I_A} k_f R_{56} \int_0^L ds \, \frac{4\pi \, Z(k_0;s)}{Z_0} \exp\left(-\frac{1}{2} \left(k_f R_{56} \sigma_\delta\right)^2\right)$$

(assuming initial Gaussian uncorrelated energy distribution)

E. L. Saldin, E. A. Schneidmiller, and M.V. Yurkov, DESY Report No. TESLA-FEL-2003-02, 2003.

Microbunching gain after BC1 of LCLS

Dominated by LSC since $Z_{LSC}(k) \propto k$

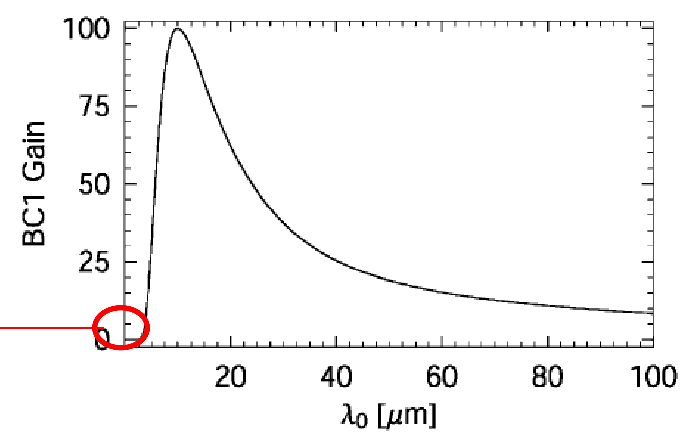

Venturini, PRSTAB 11, 030703 (2007)

Z. Huang et al., PRST-AB 7 (2004)074401

3. Experimental Observations

- COTR downstream of BC1 (compressed beam)

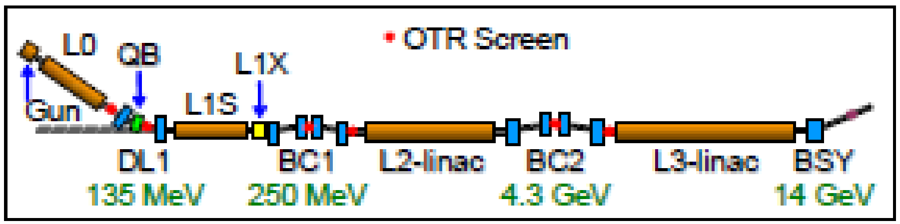

Figure 1: Layout of the LCLS accelerator.

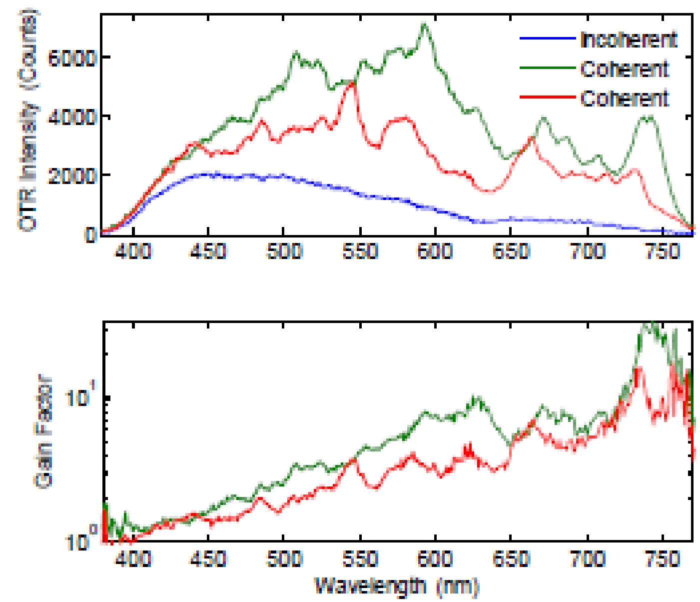

Figure 6: OTR light spectra after BC1 with the beam under normal compression (red and green) and with the coherence suppressed (blue). The spectra are in the upper panel and the spectral gain factor (ratio of coherent to incoherent spectrum) in the lower one.

$E = 250$ MeV
Q= 500 pC
σ_z=800 μm

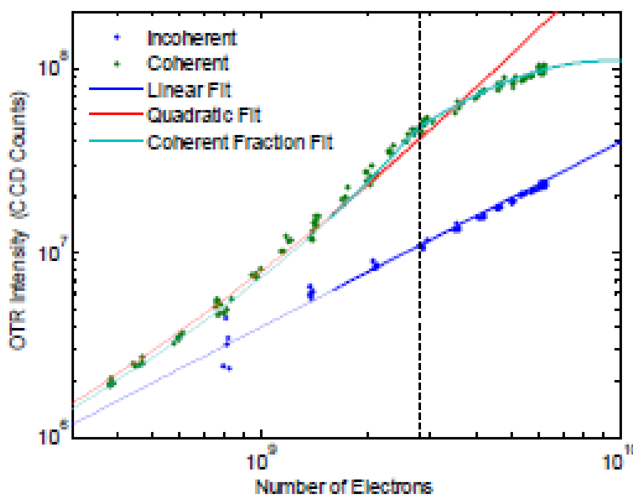

$E = 250$ MeV
Q= 250 pC
σ_z=60 μm

Fit coherent factor r in the ehancement factor

$C = \eta N + \eta N^2 r^2$ ➡ $rN = 10^4$ out of $N = 3 \times 10^9$ Loos *et al.*, FEL08

Microbunching Observed at FLASH

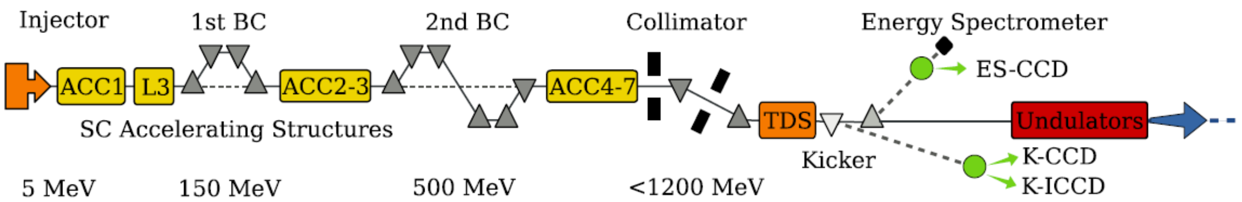

FIG. 1. Schematic layout of the Free-Electron Laser in Hamburg (FLASH) with its superconducting (SC) accelerating structures (ACC), the two magnetic bunch compressor (BC) chicanes, and the third-harmonic rf linearizer system (L3). The positions of the experimental setups and diagnostics used for the measurements presented in this paper are indicated by green dots.

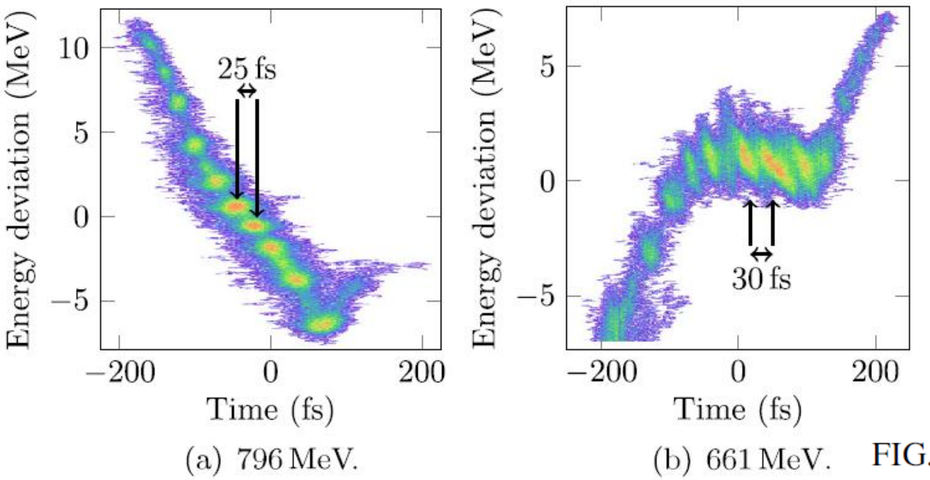

Longitudinal phase space show microbunching structure in infrared wavelength

FIG. 3. Longitudinal phase space measurements upstream of the undulators at ES-CCD for two different compression settings and mean energies: (a) 796 MeV and (b) 661 MeV. The density modulations indicate microbunching in the time-domain with periods of ~25 fs and 30 fs, respectively.

Behrens *et al*., PRSTAB 15, 062801 (2012)

4. Refining the MBI Modeling: Theories and Simulations

Goals:

- Accurate 3D force model $\vec{F} = e(\vec{E} + \vec{\beta} \times \vec{B})$
- Fully self-consistent particle dynamics
- High resolution of microbunching with shot noise

Space Charge

- Effect of 3D distribution on LSC Force
- Shot noise effect on space charge modeling

COTR downstream of LCLS dogleg (non-compressed beam)

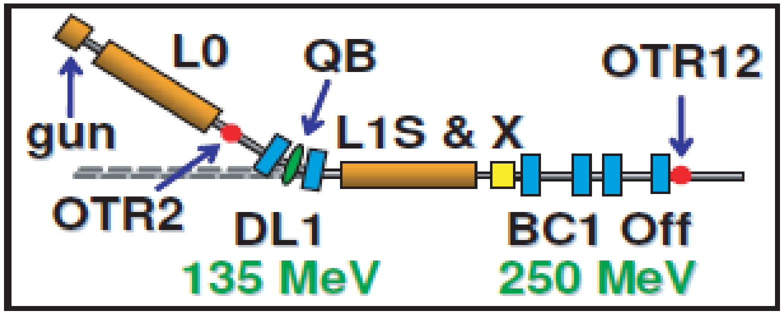

Figure 1: LCLS injector layout showing OTR2, DL1 and OTR12 for the COTR experiment when BC1 is off.

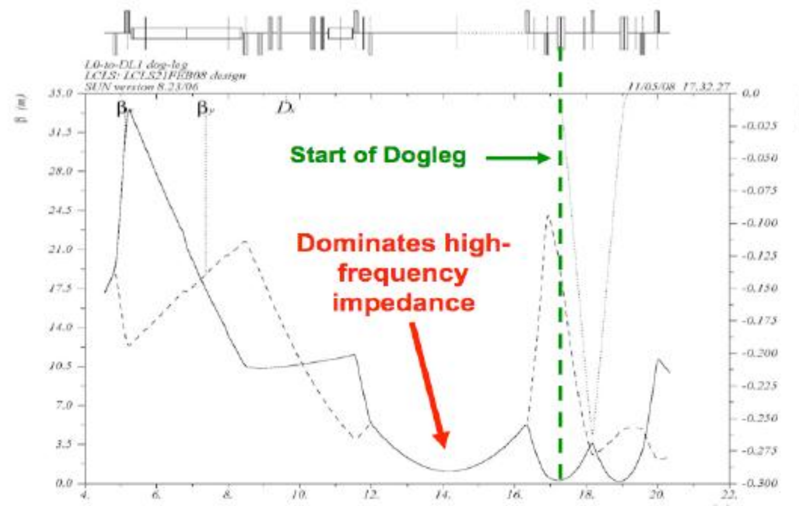

$E = 135$ MeV
$\beta_0 = 1.2$ m
R_{56}=6.3 mm
Q= 250 pC
σ_z=750 μm

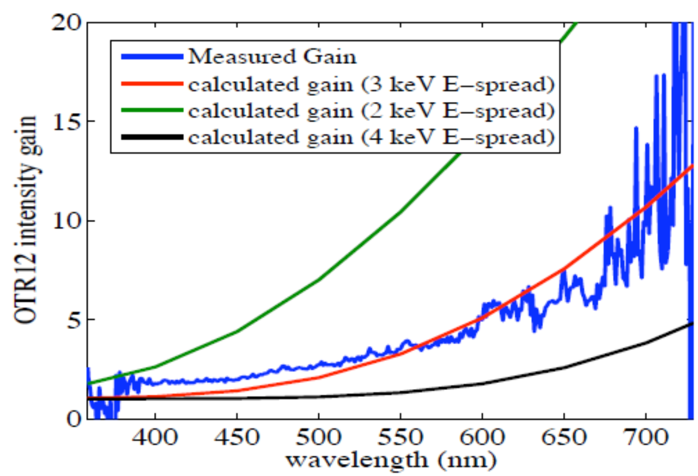

Ratner, Huang and Chao, SLAC-Pub-13392

3D Space Charge Effects on MBI

(Ratner, Chao and Huang, FEL08)

- 1D space charge impedance is not adequate for high frequency μBI, such as amplification of shot noise.
- 3D space charge field

$$E_z(x) = \frac{e}{4\pi\epsilon_0}\sum_j^N \frac{\gamma_0(z-z_j)}{[(x-x_j)^2+(y-y_j)^2+\gamma_0^2(z-z_j)^2]^{3/2}}$$

$$\tilde{E}_k(r) = \frac{-eik}{2\pi\gamma_0^2\epsilon_0}\sum_j^N e^{-ikz_j} K_0\left(\frac{k|r-r_j|}{\gamma_0}\right)$$

calculate $\langle E_k(r_1)E_k^*(r_2)\rangle$

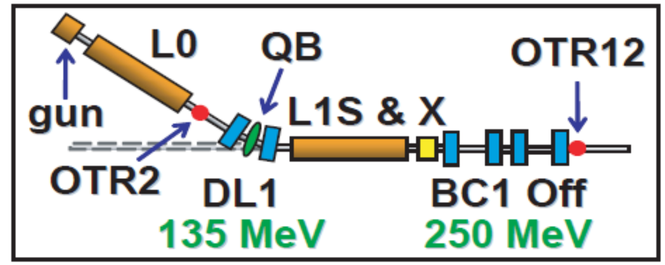

- Bunching factor in OTR observation angle

$$b(k) = \frac{1}{N}\sum_{j=1}^N e^{-ik\cdot x(X_{0j})}$$

Transverse Landau damping

$$\langle |b_c(k)|^2\rangle \approx \frac{4}{3N}\left[\frac{I_0(z_0)}{\gamma_0 I_A}\frac{R_{56}L_d}{\sigma_{x0}^2}\right]^2 \times \frac{\exp\left[-k^2R_{56}^2\sigma_{\delta0}^2 - k^2(R_2^2+\theta_y^2R_{34}^2)\sigma_{x0}^2\right]}{[1+\gamma_0^2(R_1^2+\theta_y^2R_{33}^2)]^2}$$

LSC cutoff $1/\gamma$

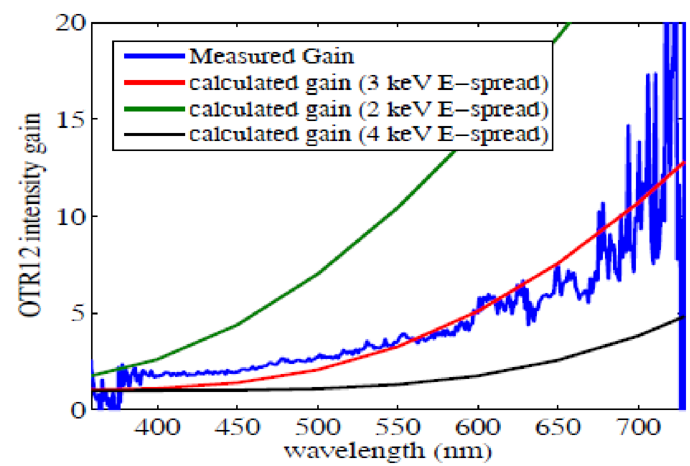

Figure 3: Measured and calculated OTR intensity gain for 250 pC charge at OTR12 as a function of the optical wavelength.

- OTR Intensity

$$\frac{d^2W}{d\omega d\Omega} = \left(\frac{d^2W}{d\omega d\Omega}\right)_1 [N + N^2|b_c(k)|^2]$$

Assumption: transverse laminar beam

More on 3D LSC: Venturini, PRSTAB, 2008

Ratner 's PhD thesis, 2010

High Resolution Simulation --- IMPACT

Qiang et al. , PRSTAB 12, 100702 (2009)

- Collective effects include
  -RF wakefield in linac
  -3D space charge
    Poisson equation using convolution of charge density with Green's function
    integrated Green function method with FFT
    Lorentz transform.
  -1D CSR in chicane (low pass filter)

- Consideration:
  -noise artificially amplified by $\sqrt{N/N_{mp}}$

- Results:
  -100M particles is needed to control shot noise and avoid over-estimation of uBI
  -effect of initial uncorrelated energy spread
  -grid size can smear microbunching instability

Simulation results for FERMI@ELETTRA FEL linac

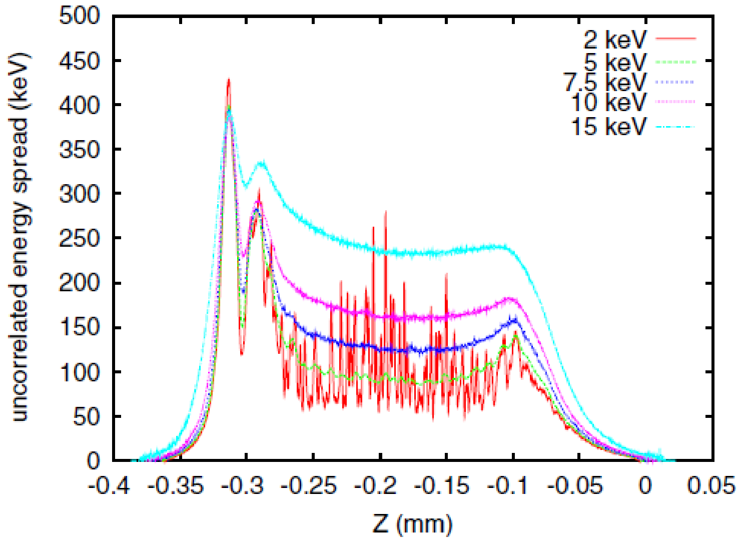

Other codes for LSC simulation: ASTRA, Elegant

Dependence on Simulation Parameters

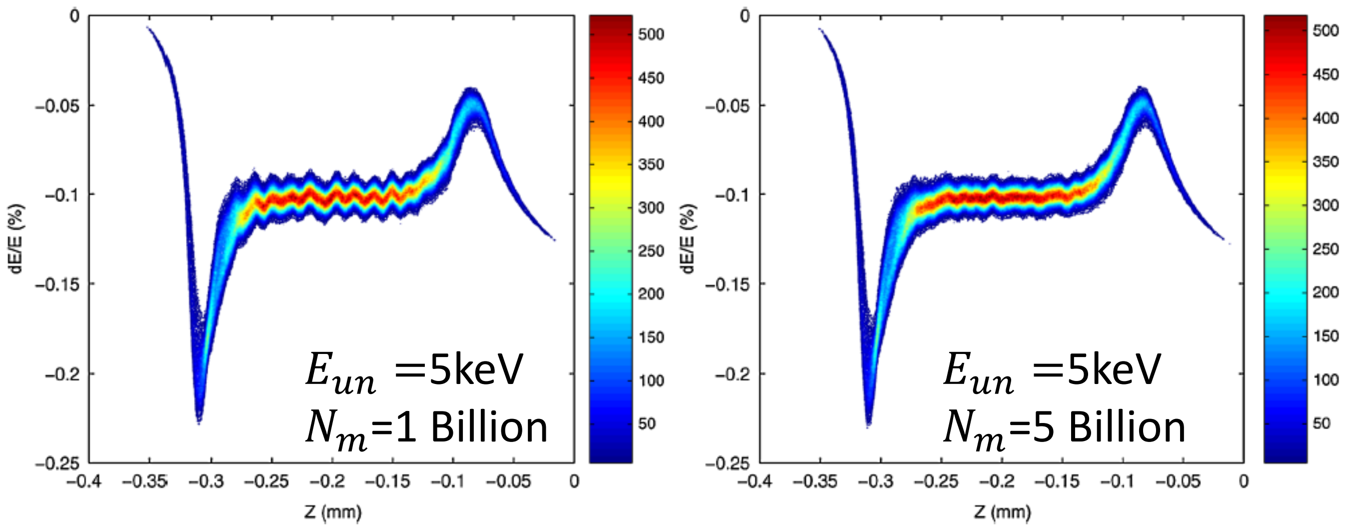

FIG. 11. (Color) Longitudinal phase space at the end of the linac using one billion (left) and five billion macroparticles (right) with an initial 5 keV rms uncorrelated energy spread.

- The gain of microbunching depends sensitively on the parameters used in the simulation, such as grid size, and number of macroparticles

- This poses big challenge for the numerical modeling of the microbunching instability

CSR Theory and Simulation

- 1D finite energy and short range effect
- Waveguide boundary condition
- 2D effect
- 3D modeling

Improved 1D CSR Force Model

- Exact 1D CSR Model Mayes and Hoffstaetter, PRSTAB 12, 024401 (2009)

Using Jefimenko's form of Maxwell equation instead of Lienard-Wiechert fileds

$$\mathbf{E}(\mathbf{x},t) = \frac{1}{4\pi\epsilon_0}\int d^3x'\left[\frac{\mathbf{r}}{r^3}\rho(\mathbf{x}',t') + \frac{\mathbf{r}}{cr^2}\partial_{t'}\rho(\mathbf{x}',t') - \frac{1}{c^2 r}\partial_{t'}\mathbf{J}(\mathbf{x}',t')\right]_{t'=t-}$$

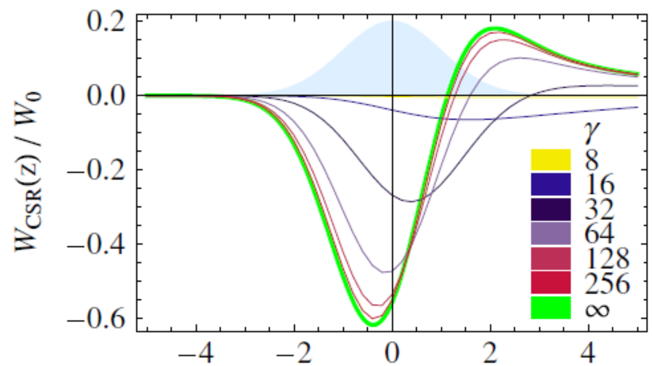

-No need for large γ or small angle approximation
-Regularization by removing space charge term
-Also include transient and shielding effects

- 1D CSR Model including short range effects (Ryne et al., 2012)

$\mu \sim (3\gamma^3/2\rho)\ s$

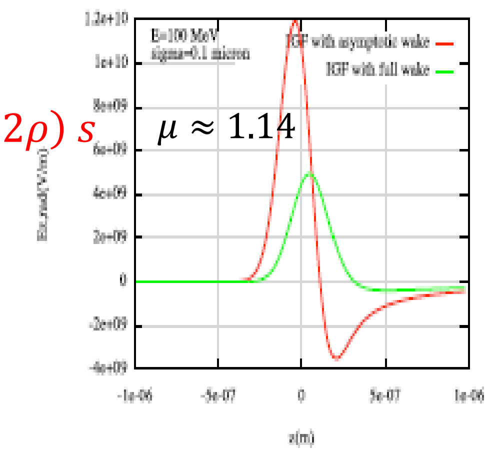

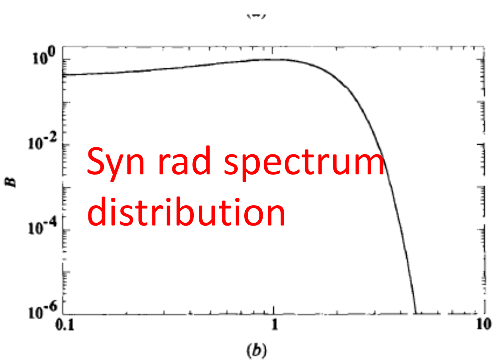

-use integrated Green's function
-important for low energy or short wavelength, such as shot noise

$$\lambda_c = 2R/3\gamma^3$$

- Extended 1D CSR Method Sagan *et al.*, PRSTAB 12, 040703 (2009)

CSR Simulation with Waveguide Boundary Conditions

Agoh and Yokoya, 2004
Gillingham and Antonsen, 2007
Zhou, IPAC 12, 2012

- Simplify Maxwell equation with paraxial approximation for $\vec{E}_{\perp}$, express $(\vec{E},\vec{B})$ in terms of $\vec{E}_{\perp}$=(E_x,E_y)

$$2ik\frac{\partial \boldsymbol{E}_{\perp}}{\partial s}+\left\{\boldsymbol{\nabla}_{\perp}^{2}+2k^{2}\left(\frac{x}{\rho}-\frac{1}{2\gamma^{2}}\right)\right\}\boldsymbol{E}_{\perp}=\mu_{0}\boldsymbol{\nabla}_{\perp}J_{0},$$

- Solve Parabolic wave equation using finite difference method or spectral method
- Include waveguide boundary conditions
- Backward propagating wave ignored

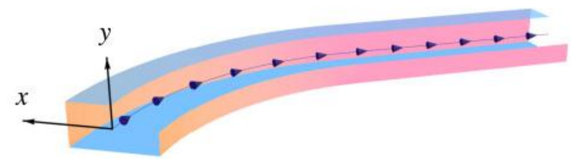

❑ Comparison of the SR impedance and Measured incoherent SR power spectrum at NSLS VUV ring

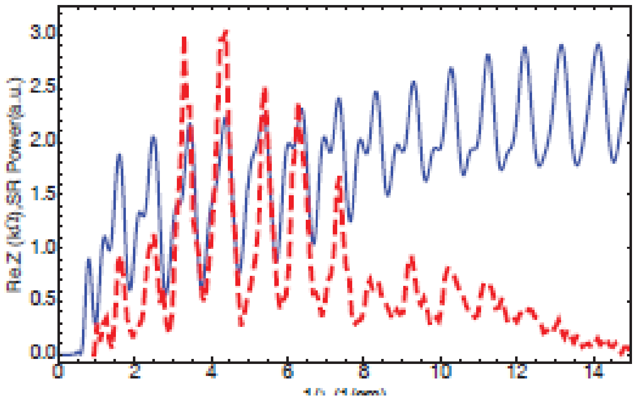

Self-Consistent 2D Mean Field Treatment

Bassi et al., PRSTAB 12 (2009)

- Solve Vlasov-Maxwell system

$$\mathcal{F} = (E_Z, E_X, B_Y)^T \qquad \mathbf{S}(\mathbf{R}, u) = Z_0 Q \begin{pmatrix} c\partial_Z \rho_L + \partial_u J_{L,Z} \\ c\partial_X \rho_L + \partial_u J_{L,X} \\ \partial_X J_{L,Z} - \partial_Z J_{L,X} \end{pmatrix}$$

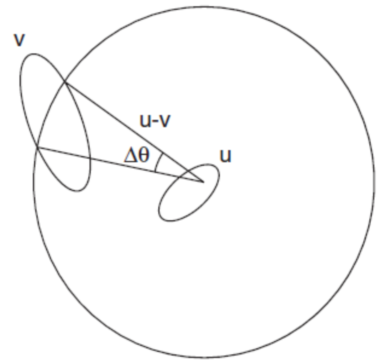

Find EM fields from 2D numerical integration:

$$\mathcal{F}(\mathbf{R}, Y, u) = -\frac{1}{4\pi} \int_{\mathbb{R}^2} d\mathbf{R}' \int_{\mathbb{R}} dY' \xi(Y') \frac{\mathbf{S}\{\mathbf{R}', u - [|\mathbf{R}' - \mathbf{R}|^2 + \eta^2]^{1/2}\}}{[|\mathbf{R}' - \mathbf{R}|^2 + \eta^2]^{1/2}}$$

Monte-Calo representation: charge density constructed from Fourier series noise reduction

Dynamic advances: interaction picture in beam frame, self-consistent

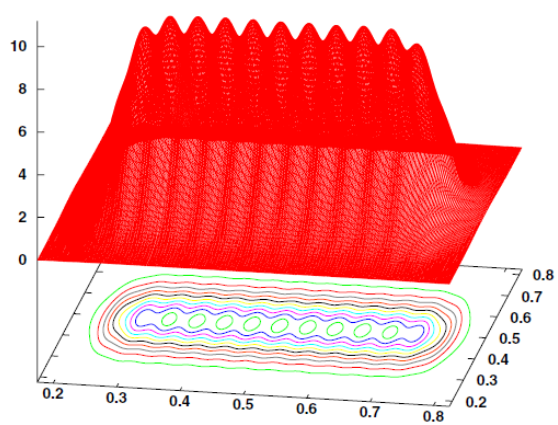

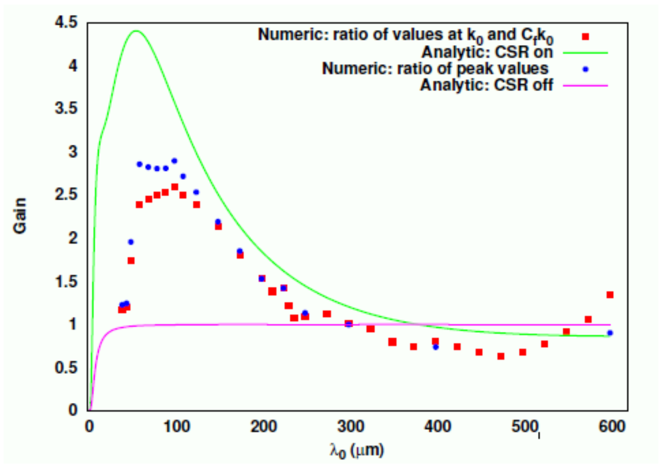

3D CSR Simulation using Lienard-Wiechert Approach

Ryne et al., 4th microbunching workshop

- 3D Lienard-Wiechert code
- Numerically solve retarded time
- Not self-consistent yet

$$\vec{E} = \left[\frac{q}{\gamma^2 \kappa^3 R^2} (\hat{n} - \vec{\beta}) + \frac{q}{\kappa^3 R c} \hat{n} \times \left\{ (\hat{n} - \vec{\beta}) \times \frac{\partial \vec{\beta}}{\partial t} \right\} \right]$$

- Use 6.24 Billion electrons, 1GeV bunch show bigger noise in Ez_rad

- study shot-noise effects by using a real-world # of electrons

At fixed energy, shot noise goes down with increasing # of particles

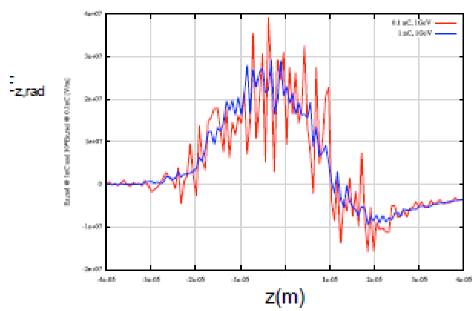

$E_{z,rad}$ at the centroid of a 1 GeV bunch with # of electrons = 624 million (0.1nC) and 6.24 billion (1 nC) (0.1nC data scaled by 10x)

At fixed # of particles, shot noise increases with energy

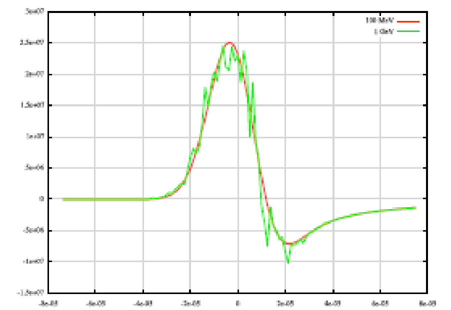

$E_{z,rad}$ at the centroid of a 1 nC bunch with energy 100 MeV and 1 GeV

imagine a billion ultra-narrow flashlight beams shining on each other

besides difficult-to-model spatial dependence, also need to take into account finite speed of light

4. Mitigation Method and Applications

- Mitigation
  - Laser heater
  - Reversible heater
- Application
  - LSC amplifier
  - Cooling ion beam

Mitigation I: Laser Heater

Z. Huang et al., PRST-AB 7 (2004)074401

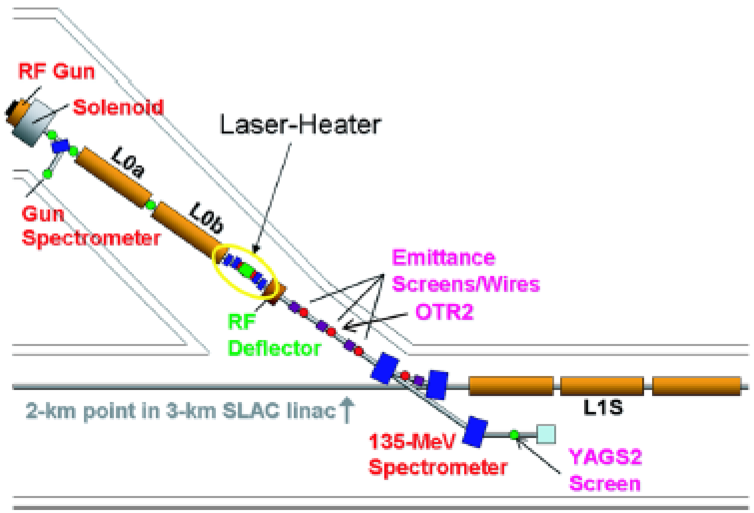

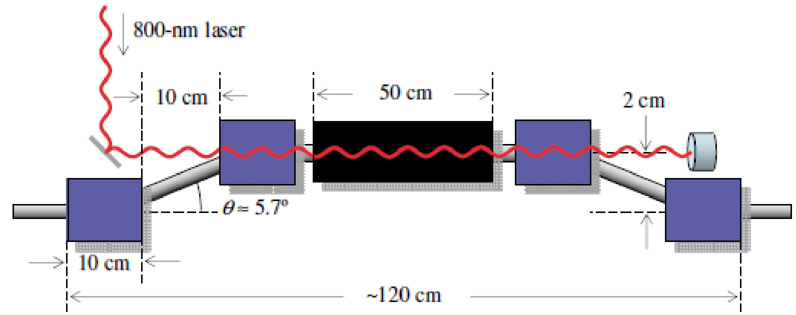

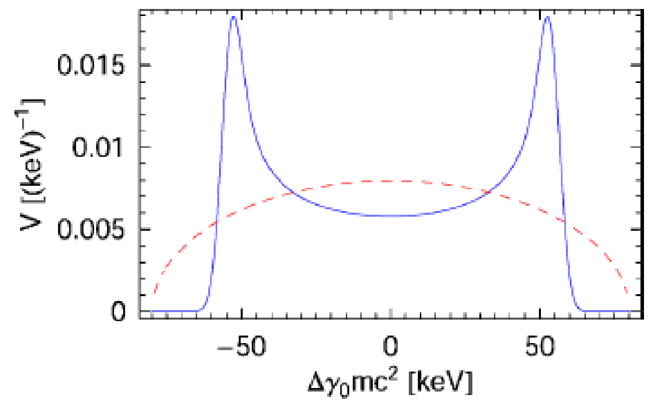

Introduce uncorrelated energy spread

$$\Delta\gamma_L(r) = \sqrt{\frac{P_L}{P_0}\frac{KL_u}{\gamma_0\sigma_r}}\left[J_0\left(\frac{K^2}{4+2K^2}\right)-J_1\left(\frac{K^2}{4+2K^2}\right)\right]\exp\left(-\frac{r^2}{4\sigma_r^2}\right),$$

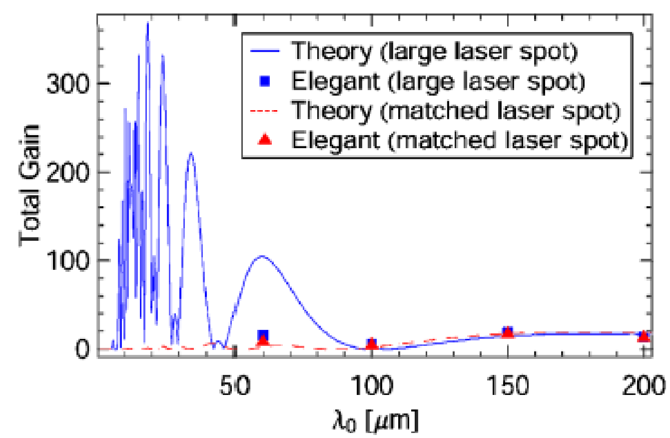

Gain for the laser heater

$$G = \left|\frac{b_f}{b_0}\right| \approx \frac{I_0}{\gamma I_A}\left|k_f R_{56}\int_0^L ds\,\frac{4\pi Z(k_0;s)}{Z_0}\right|\left|\int d\delta_0 V(\delta_0)\, e^{-ik_f R_{56}\delta_0}\right|.$$

Laser-induced energy modulation used to suppress uBI at LCLS in x-ray FEL, but COTR interferences still exist.

Laser Heater Off

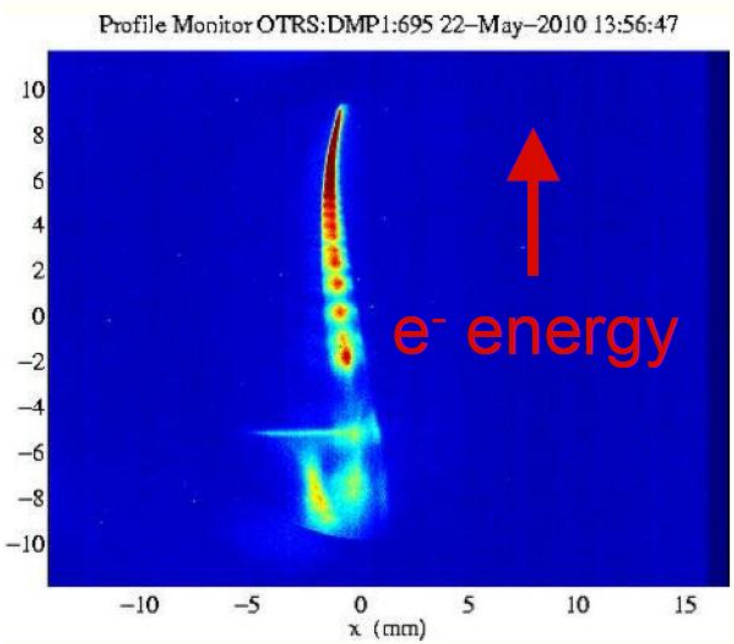

Dump YAG Screen

J. Welch et al., FEL10

Laser Heater ON – No Instability

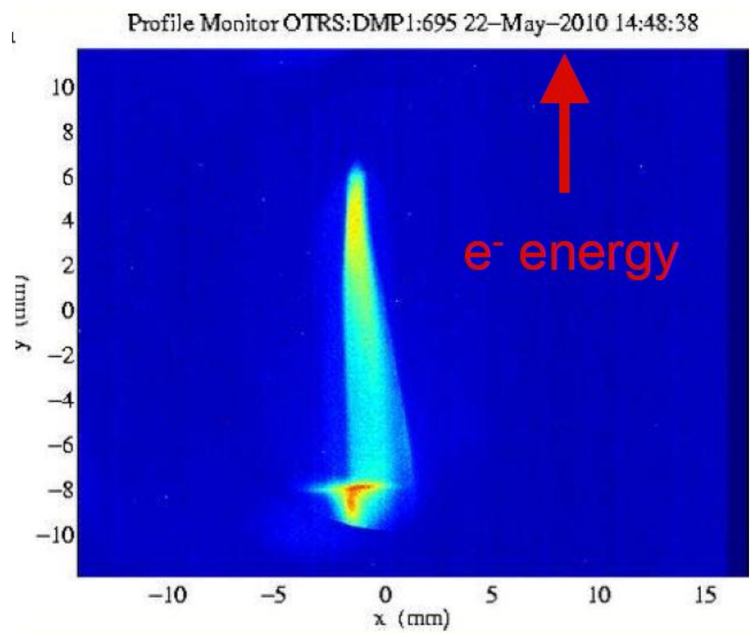

Mitigation II: Reversible Heater

Behrens, Huang, Xiang, PRSTAB 15, 022802 (2012)

- Use transverse deflecting structure to deflect beam vertically
- Induce energy spread according to Panofsky-Wenzel theory

$$\boxed{\Delta \vec{p}_\perp = -i\frac{e}{\omega}\int_0^L \nabla_\perp \mathcal{E}_z d\tilde{z},}$$

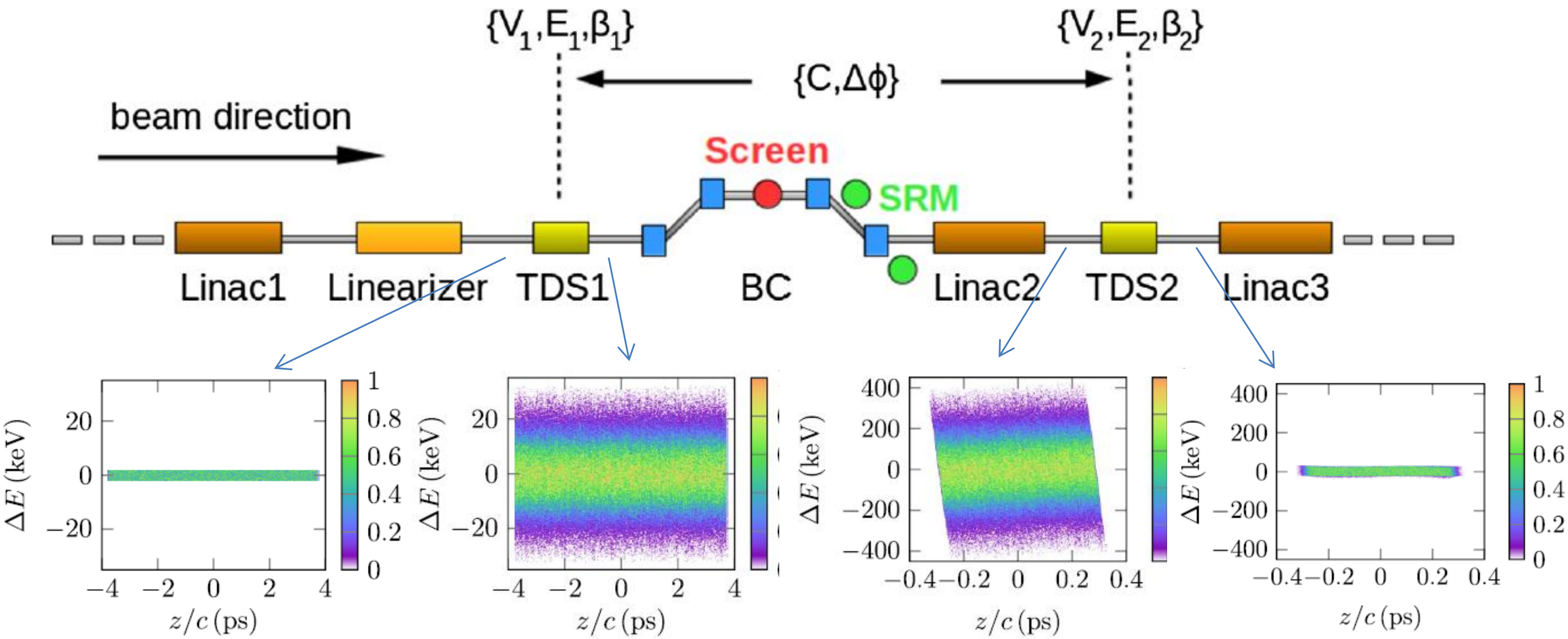

(a) Upstream of TDS1. (b) Downstream of TDS1. (c) Upstream of TDS2. (d) Downstream of TDS2.

Simulation of Suppression of μBI using reversible heater

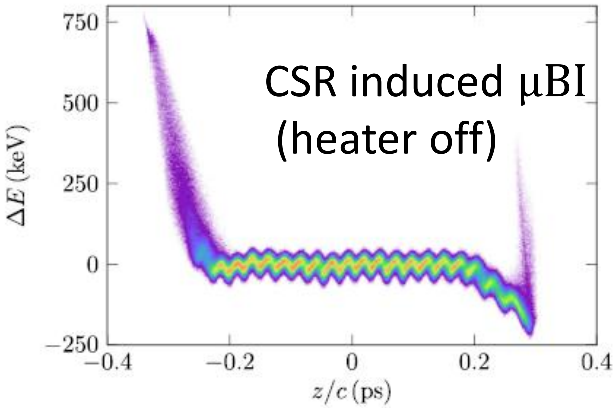

(a) Downstream of TDS2: Heater system off.

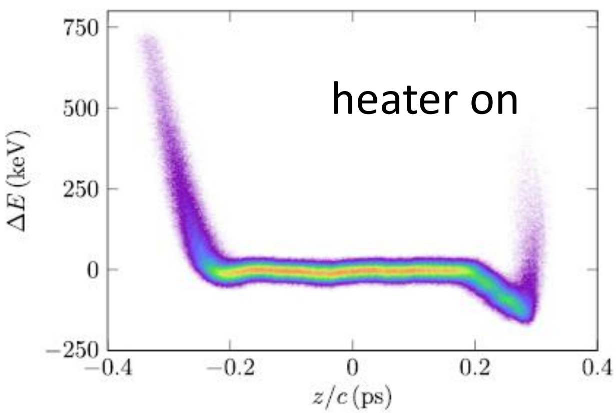

(b) Downstream of TDS2: Heater system on.

FIG. 7. Simulation on suppression of microbunching instabilities due to an initial density modulation, i.e., simulating CSR-driven microbunching. The entire longitudinal phase space, after removing the correlated energy chirp, is shown.

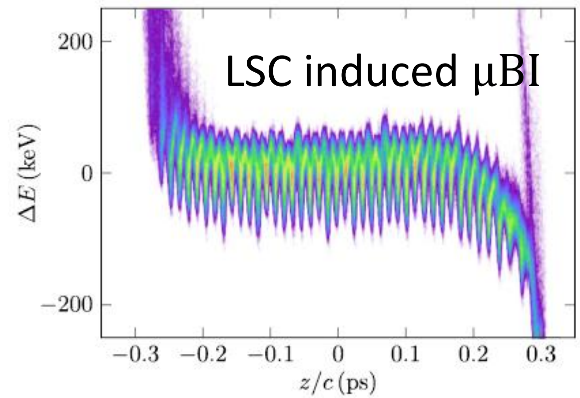

(a) Downstream of TDS2: Heater system off.

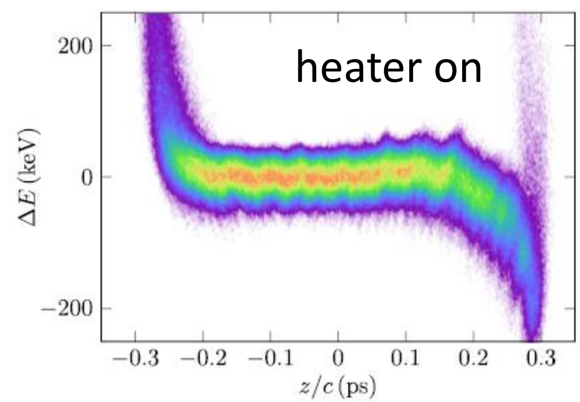

(b) Downstream of TDS2: Heater system on.

FIG. 8. Simulation on suppression of microbunching instabilities due to an initial energy modulation, i.e., simulating longitudinal space charge driven microbunching. For the sake of clarity, only the core of the longitudinal phase space, after removing the correlated energy chirp, is shown.

Application I: Longitudinal Space Charge Amplifier

Schneidmiller and Yurkov, PRSTAB 13, 110701 (2010)

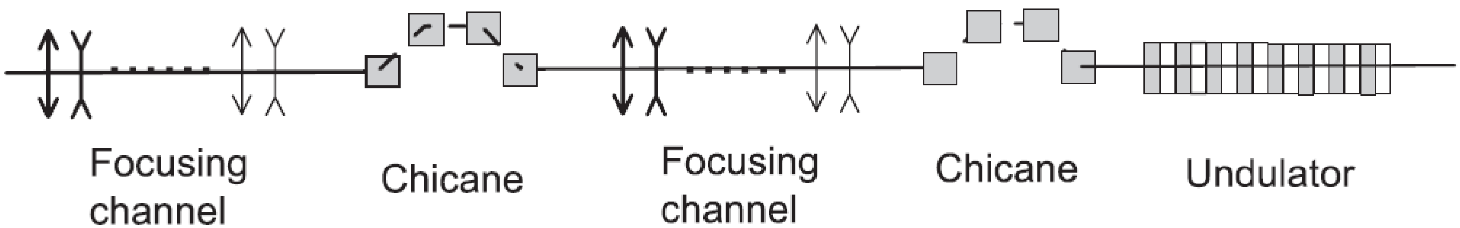

- **Gain for each stage:** $$G_n = Ck|R_{56}|\frac{I}{\gamma I_A}\frac{4\pi|Z(k)|L_d}{Z_0}\exp\left(-\frac{1}{2}C^2k^2R_{56}^2\frac{\sigma_\gamma^2}{\gamma^2}\right).$$

$$\frac{4\pi Z(k)}{Z_0} = \frac{ik}{\gamma_z^2}\left(2\ln\frac{\gamma_z}{k\sigma_\perp} + \mathrm{const}\right)$$

Impedance maximum at: $\lambda \simeq \lambda_{\rm opt} \simeq \frac{\sigma_\perp}{\gamma_z} = \frac{\sqrt{\epsilon\beta}}{\gamma_z}$, Optimal R_{56} at: $R_{56} \simeq \lambda\frac{\gamma}{\sigma_\gamma}$

- **Length constraint:** $L_d \leq \min(L_1, L_2).$

  L_1 is the wavelength of plasma oscillation
  L_2 is the length for velocity spread due to emittance to spoil the modulation

- **Total gain:** $G_{\rm tot} = G_1G_2\ldots G_n$
- **Broadband amplification**

Example of LSC Amplifier

Dohlus, Schneidmiller and Yurkov, PRSTAB 13, 110701 (2010)

$\mathrm{E} = 1.2\ \mathrm{GeV}$
$\epsilon_n = 0.4\ \mathrm{mm-mrad}$
R_{56}=7.1 μm
L_d = 2.8 m
Q= 100 pC
L_tot =3.5 m x3=14 m

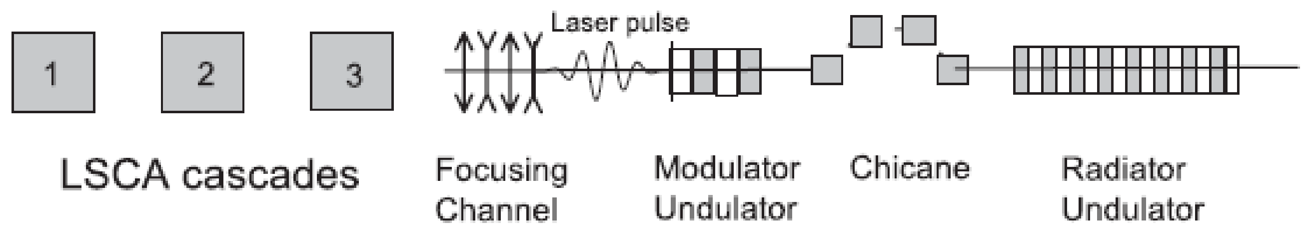

Generation of attosecond soft x-ray pulses
(50 attosecond duration, $\lambda = 4\ nm$)

- A short slice of electron bunch gets the strongest energy chirp
- And being strongly compressed
- Amplification through last chicane optimal

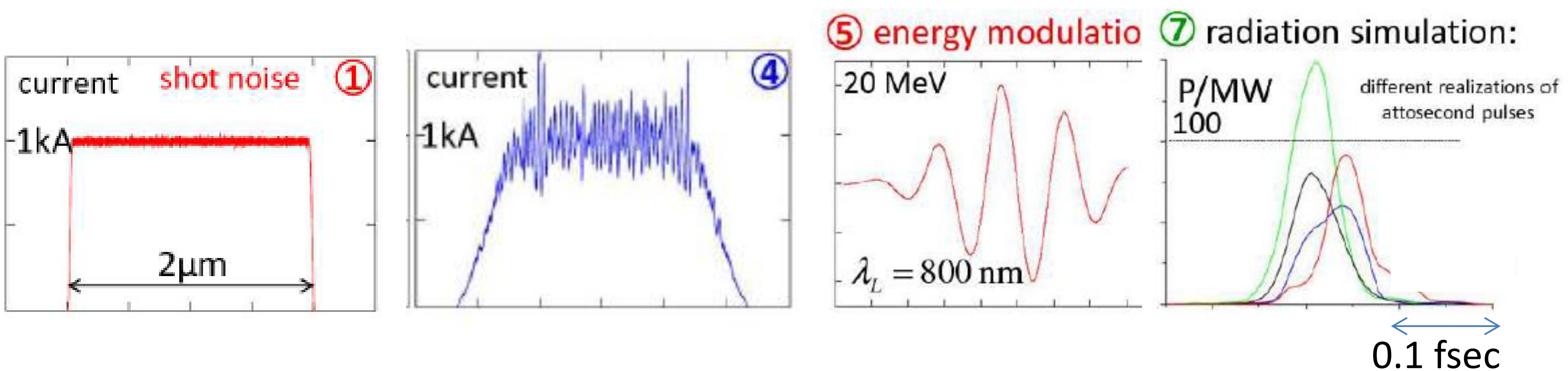

Application II: Microbunched Electron Cooling (MBEC) for Ions

Ratner, SLAC-PUB-15346 (2013)

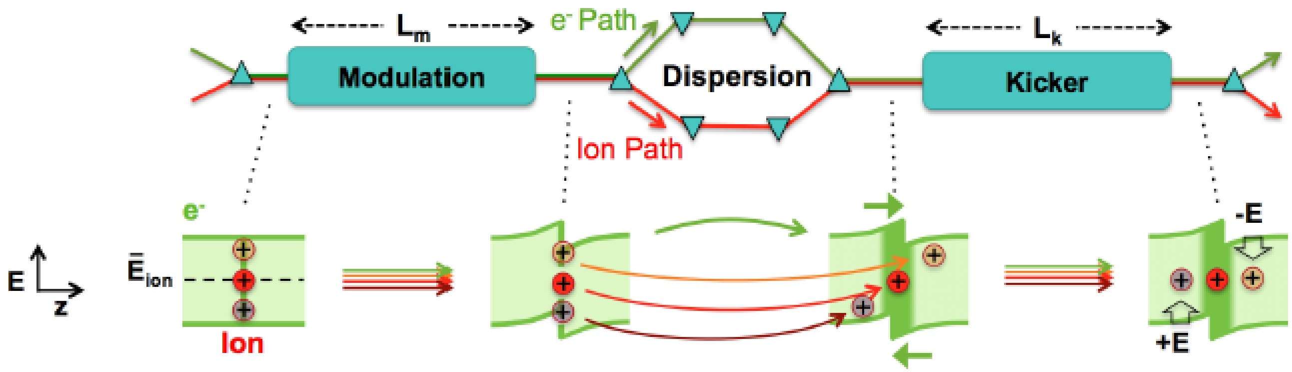

1. Ion Imprints on Electrons

2. Bunching mechanism

3. Energy Correction

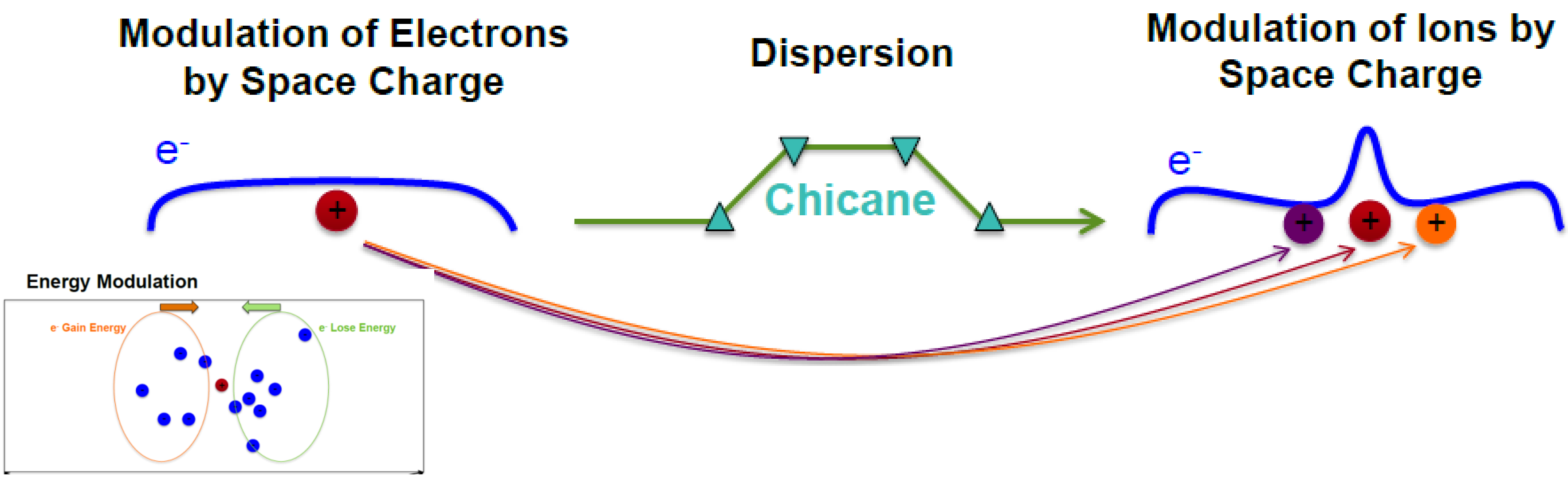

Multi-Stage Microbunching

Ratner, 5th microbunching workshop

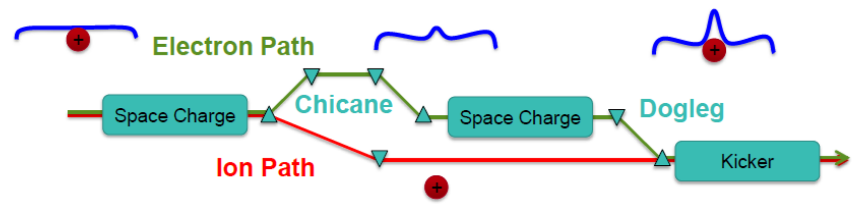

Simulation: LHC 7 TeV

	Stage 1	Stage 2-5	Kicker
Relativistic factor (γ)	7000		
Current (I)	100 A		
Energy spread	$5\mathrm{x}10^{-6}$ (20 keV)		
Beam radius (a)	100 μm	50 μm	100 μm
Dispersion (R_{56})	100 μm	4 x -25 μm	N.A.
Interaction Length (L_m)	25 m	4 x 12.5 m	25 m
LHC energy spread (σ_E)	800 MeV		

40 MHz
100 ps

IBS growth time: 2hr including errors

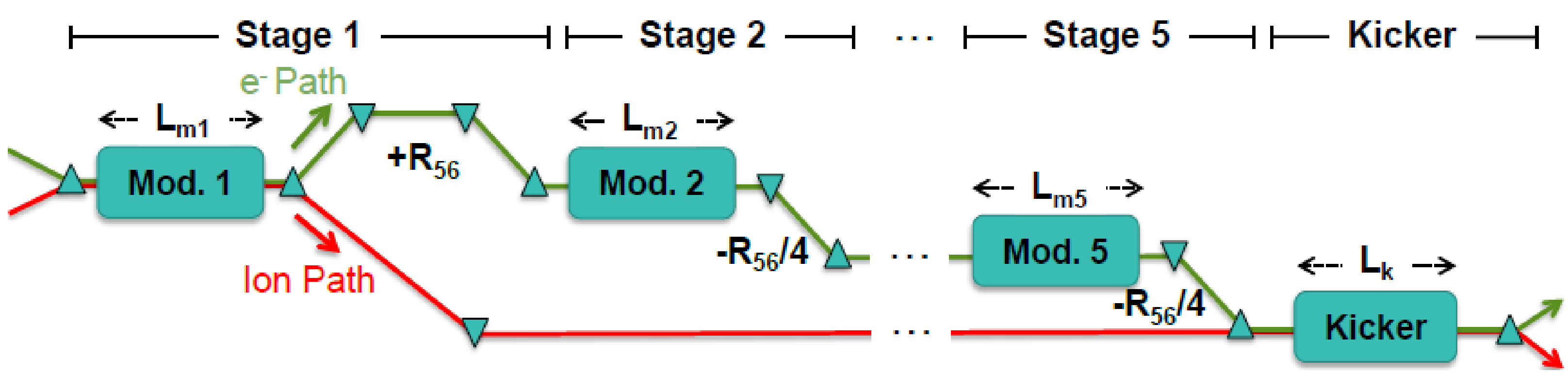

Takes 30 million turns ~ 1 hour to shift by 800 MeV

Summary

- 1D models of the μBI theory and simulations have laid foundation for further development of μBI
- Many new development of theory and simulation are made to refine the bunch shot noise description and also more complete force modeling
- Challenges remain in the front of fully self-consistent simulation at short wavelength
- Mitigation schemes are implemented, and applications of μBI are being proposed and to be tested
- μBI plays a critical role in MEIC cooler design, we need a thorough study to get it under control. It is interesting that it is now proposed to work for cooling.

Thank you for your attention!